

# Contribution of Linear Free Energy Relationships to Isozyme- and pH-Dependent Substrate Selectivity of Glutathione S-Transferases: Comparison of Model Studies and Enzymatic Reactions

Brenda S. Nieslanik and William M. Atkins\*

Department of Medicinal Chemistry, Box 357610, University of Washington, Seattle, Washington 98195-7610

Received March 11, 1998

**Abstract:** A novel application of linear free energy relationships is described in which the substrate selectivities and pH dependencies of glutathione S-transferases (GSTs) are correlated to the  $pK_a$  of glutathione (GSH) at the active site. To determine whether the variation in the thiol  $pK_a$  of GSH at the active sites of GST isozymes can contribute to their differential selectivity for electrophilic substrates, model studies were performed with 4-substituted thiobenzenes, with  $pK_a$  values ranging from 4.5 to 7.5. Second-order rate constants were determined for the specific base-catalyzed reaction of each thiol with a diverse range of GST electrophilic substrates. Brønsted coefficients ( $\beta_{nuc}$ ) for these reactions in 10% DMF:90% H<sub>2</sub>O were determined for each electrophile;  $\beta_{nuc}$  ranged from 0.16 to 0.93. In 30% DMF:70% H<sub>2</sub>O, the  $\beta_{nuc}$  values increased relative to 10% DMF and ranged from 0.29 to 1.04. Numerical simulations demonstrate that these ranges of  $\beta_{nuc}$  values along with the isozyme-dependent variation in GSH  $pK_a$  could account for a 7.5-fold difference in relative turnover rates for GST catalysis of some electrophilic substrates. To challenge the predictions of this Brønsted analysis, electrophiles for which chemical steps are rate limiting in enzyme turnover were used as a substrate in reactions with a series of GSTA1-1 mutants with variable GSH  $pK_a$ .  $\beta_{nuc}$  values were determined to be  $0.16 \pm 0.05$  for cumene hydroperoxide (CHP) and  $0.25 \pm 0.06$  for 1-chloro-2,4-dinitrobenzene, in excellent agreement with the model studies. Furthermore, the dependence of the relative rates of CHP turnover on GSH  $pK_a$  was well correlated, at pH 6.5, 7.4, and 8.0 with the relative rates predicted by the Brønsted analysis. Thus, even for a reaction characterized by a low  $\beta_{nuc}$  value, variation of the  $pK_a$  of enzyme-bound GSH leads to changes in the intrinsic reactivity of the nucleophilic GS<sup>-</sup>, according to the Brønsted free energy relationship. In principle, variation of the  $pK_a$  of GSH may contribute to isozyme-dependent substrate selectivity.

The cytosolic glutathione S-transferases (GSTs)<sup>1</sup> are a family of detoxication enzymes that catalyze the conjugation of glutathione (GSH) with various endogenous and xenobiotic electrophiles. Due to their primary role in drug metabolism and tumor drug resistance and their potential role in bioremediation, GSTs have been the recent focus of intense mechanistic and structural research.<sup>2</sup> The mammalian cytosolic GSTs are represented by five gene classes (A, P, M, K, and T) that exhibit overlapping, but distinct, selectivities for structurally diverse electrophilic substrates. High-resolution X-ray structures of isozymes of each gene class, in various ligand states, have facilitated structure/function comparisons between isozymes and classes.<sup>3</sup> Each of the cytosolic GSTs has a catalytic tyrosine or serine at the active site that hydrogen bonds to the thiol of

GSH. In addition, spectroscopic and kinetic data yield a  $pK_a$  for enzyme-bound GSH of 6.5–7.4, in contrast to the  $pK_a$  of thiols in solution, 9.3.<sup>4</sup> The catalytic advantage appears obvious because the thiolate anion is a more reactive nucleophile than the protonated thiol. In addition, it was appreciated long ago that the selectivity for electrophilic substrates varies between GST isozymes,<sup>5</sup> and the available X-ray structures clearly suggest that the active site topologies of GST isozymes are likely to contribute to relative activities toward different substrate electrophiles. In light of results recently obtained, however,

\* Corresponding author phone: (206) 685-0379. Fax: (206)685-3252. E-mail: winku@u.washington.edu.

(1) Abbreviations: CHP, cumene hydroperoxide; CDNB, 1-chloro-2,4-dinitrobenzene; DMF, dimethylformamide; E, an electrophile reactant of glutathione conjugation; EPNP, 1,2-epoxy-3-(*p*-nitrophenoxy)propane; EtOH, ethanol; FAB, fast atom bombardment mass spectrometry; *trans*-PBO, *trans*-4-phenyl-3-buten-2-one; GST, glutathione S-transferase; GSH, glutathione; GS<sup>-</sup>, the thiolate anion of GSH; [GST·GSH·E], the ternary complex formed from GST, GSH, and an electrophile; [GST·GS<sup>-</sup>·E], the ternary complex of GST, GS<sup>-</sup>, and E; 2-NP, 2-nitropropane; MES, 2-(*N*-morpholino)ethanesulfonic acid; **1**, 4-methoxybenzenethiol; **2**, 4-methylbenzenethiol; **3**, 4-hydroxybenzenethiol; **5**, 4-chlorobenzenethiol; **6**, 4-nitrobenzenethiol.

(2) (a) Rushmore, T. H.; Pickett, C. B. *J. Biol. Chem.* **1993**, *268*, 11475. (b) Armstrong, R. N. *Adv. Enzymol. Relat. Areas Mol. Biol.* **1994**, *69*, 1. (c) Hayes, J. D.; Pulford, D. J. *CRC Biochem. Mol. Biol.* **1995**, *30*, 445.

(3) (a) Armstrong, R. N. *Chem. Res. Toxicol.* **1997**, *10*, 2. (b) Sinning, P.; Kleywegt, G. J.; Cowan, S. W.; Reinemer, P.; Dirr, H. W.; Huber, R.; Gilliland, G. L.; Armstrong, R. N.; Ji, X.; Board, P. G.; Olin, B.; Mannervik, B.; Jones, T. A. *J. Mol. Biol.* **1993**, *232*, 192. (c) Wilce, M. C. J.; Board, P. G.; Feil, S. C.; Parker, M. W. *EMBO J.* **1995**, *14*, 2133. (d) Ji, X.; Zhang, P.; Armstrong, R. N.; Gilliland, G. L. *Biochemistry* **1992**, *31*, 10169. (e) Bjornstedt, R.; Stenberg, G.; Widersten, M.; Board, P. G.; Sinning, I.; Jones, T. A.; Mannervik, B. *J. Mol. Biol.* **1995**, *247*, 765.

(4) (a) Graminski, G. F.; Kubo, Y.; Armstrong, R. N. *Biochemistry* **1989**, *28*, 3562. (b) Kong, K. H.; Takasu, K.; Inoue, H.; Takahashi, K. *Biochem. Biophys. Res. Commun.* **1992**, *184*, 194. (c) Dietze, E. C.; Ibarra, C.; Dabrowski, M. J.; Bird, A.; Atkins, W. M. *Biochemistry* **1996**, *35*, 11938. (d) Liu, S.; Zhang, P.; Ji, X.; Johnson, W. W.; Gilliland, G. L.; Armstrong, R. N. *J. Biol. Chem.* **1992**, *267*, 4296. (e) Huskey, S.-E.; Huskey, W. P.; Lu, A. Y. H. *J. Am. Chem. Soc.* **1991**, *113*, 2283. (f) Liu, S.; Ji, X.; Gilliland, G. L.; Stevens, W. J.; Armstrong, R. N. *J. Am. Chem. Soc.* **1993**, *115*, 7910.

(5) (a) Habig, W. H.; Pabst, M. J.; Jakoby, W. B. *J. Biol. Chem.* **1974**, *249*, 7130. (b) Mannervik, B.; Danielson, U. H. *CRC Crit. Rev. Biochem.* **1988**, *23*, 283. (c) Mannervik, B. *Adv. Enzymol. Mol. Biol.* **1985**, *57*, 357.

we examine here the possibility that differential reactivity of GST isozymes toward different electrophiles, E, may result also from different inherent nucleophilicity of the thiolate anion in the ternary complex [GST·GS<sup>-</sup>·E], as predicted by Brønsted behavior. This analysis yields a novel perspective of GST substrate specificity and pH vs rate profiles based on a 'classical' free energy relationship.

Several investigators<sup>6</sup> have pointed out that the hydrogen bond between GS<sup>-</sup> and active site residues leaves the enzyme with a paradox: according to Brønsted relationships, the thiolate that is generated from GSH with a reduced pK<sub>a</sub> is predicted to be less nucleophilic than the analogous thiolate generated from a GSH with a 'normal' pK<sub>a</sub>. The Brønsted equation describing nucleophilic reactivity (eq 1), which is a variation of the original Brønsted theory for acid–base catalysis,<sup>7</sup> is one example of a linear free energy relationship in which equilibrium constants for protonation/deprotonation of a series of acids vary linearly with the rate constants, *k*, for nucleophilic reactions of their conjugate bases:

$$\log k = \beta_{\text{nuc}} pK_{\text{a}} + C \quad (1)$$

That is, as the enzyme generates more of the nucleophilic anion by reducing the pK<sub>a</sub> of GSH, the intrinsic nucleophilic reactivity of this anion also decreases by an amount determined by the β<sub>nuc</sub> value of the Brønsted relation. The situation for GST is directly analogous to the case considered many years ago for serine proteases.<sup>8</sup> As discussed previously, even if active site-imposed steric constraints were not present, then the observed rate of the enzymatic product formation, V<sub>max</sub>, between GS<sup>-</sup> and electrophile bound in the ternary complex, [GST·GS<sup>-</sup>·E], will be a complex function of the pK<sub>a</sub> of the enzyme-bound GSH, the pH, and the β<sub>nuc</sub> value for each particular GS<sup>-</sup>·E pair, where β<sub>nuc</sub> is the Brønsted coefficient for nucleophilic attack in eq 1.

Four components of the classic Brønsted relation as it applies to GST catalysis warrant reconsideration: (1) Structurally diverse electrophiles are substrates for GSTs, and hence the range of relevant β<sub>nuc</sub> values may be large. Nucleophilic attack of aliphatic thiols on electrophiles in aqueous solution is associated usually with low β<sub>nuc</sub> values.<sup>6</sup> Qualitatively, therefore, an increase in the fraction of thiolate as compared to protonated thiol that is achieved by hydrogen bonds at the active sites of GSTs is expected to offset any decrease in reactivity of the resulting thiolate anion. However, a quantitative analysis has not been performed. (2) There is a range of pK<sub>a</sub> values for GSH bound at the active sites of individual GST isozymes rather than a single value. For example, the pK<sub>a</sub> of GSH bound to the rat A 1-1 GST is 7.4, in marked contrast to the values reported for the M and P class enzymes, pK<sub>a</sub> = 6.5–6.9.<sup>4</sup> Apparently, the pK<sub>a</sub> of GSH bound to different GST isoforms varies by nearly an entire pK<sub>a</sub> unit. Therefore, even if β<sub>nuc</sub> values for GST-catalyzed reactions are small, this large range of pK<sub>a</sub> values would, in principle, contribute to differences in

reaction rates for various electrophiles bound at the active sites of individual GSTs, according to the Brønsted relation summarized above. As shown within, Brønsted relationships predict that there is an optimal thiol pK<sub>a</sub> for each electrophile. (3) The pK<sub>a</sub> that yields optimal rates for each electrophile will change with pH. To the extent that pH is variable in experiments *in vitro*, it must be considered as part of a complete Brønsted analysis for GST-dependent processes. (4) The 'nonaqueous' nature of GST active sites must be considered. It is well appreciated that solvent markedly affects β<sub>nuc</sub> values by differential effects on ground vs transition states. It is generally observed for reactions between thiolate anions and common GST substrates that, with decreasing solvent polarity, β<sub>nuc</sub> values increase.<sup>6c,9</sup> On the basis of several high-resolution crystal structures of different GSTs and solvent isotope effects,<sup>4c</sup> it is clear that in the presence of electrophilic substrates the nucleophilic thiolate is likely to experience a decreased solvent polarity as compared to aqueous solution. In turn, relevant β<sub>nuc</sub> values may be larger than observed for analogous reactions in bulk aqueous solvent. Therefore, the solvent composition was explicitly varied here, and the dependence of β<sub>nuc</sub> on macroscopic dielectric constant was determined for thiol attack on electrophilic GST substrates.

Notably, attempts to determine β<sub>nuc</sub> values for GST-catalyzed reactions with the electrophile CDNB have been made with site-directed mutants for which bound GSH has different pK<sub>a</sub> values<sup>4d,f</sup> and with synthetic GSH analogues.<sup>6b</sup> In some cases, 'abnormal' Brønsted behavior has been observed, i.e., negative β<sub>nuc</sub> values are obtained. These results have prompted widespread interest<sup>10</sup> in the factors controlling reactivity of the thiolate nucleophile. On the basis of X-ray structures of GST mutants,<sup>6a</sup> the abnormal Brønsted behavior is likely due to changes in reaction coordinate geometry or solvation upon amino acid substitutions in GST or GSH.

As described herein, we hypothesized that the variance in pK<sub>a</sub> exhibited by GSH at the active sites of different GSTs and large β<sub>nuc</sub> values expected for some electrophilic substrates under the nonaqueous solvation conditions could be sufficient to cause differences in apparent V<sub>max</sub> rates for GSH conjugation with various electrophiles at the active sites of different GST isozymes. In principle, the pK<sub>a</sub> of GSH bound to an individual GST could be optimized for reaction with a specific electrophile, at the expense of other substrates, if β<sub>nuc</sub> values differed sufficiently among electrophiles. Moreover, on the basis of the observation that the pH vs rate profiles vary with electrophile and with GST variants having different GSH pK<sub>a</sub> values, we hypothesized that Brønsted behavior contributes to the pH vs rate profiles. That is, if GSTs sample a sufficient range of β–pK<sub>a</sub>–rate space, then the pK<sub>a</sub> will be a determinant of substrate selectivity. To test these hypotheses, however, it was necessary to determine representative values of β<sub>nuc</sub> for reactions in which thiols of varying pK<sub>a</sub> attack chemically distinct electrophiles. The range of β<sub>nuc</sub> values for this series of thiols provides constraints on the β–pK<sub>a</sub>–rate space for GST-catalyzed conjugation of glutathione with different electrophilic substrates. The model reactions studied here are summarized in Figure 1, and they include thiols that exhibit a pK<sub>a</sub> range from 4.5 to 7.5, which spans the range of pK<sub>a</sub> values observed for GSH bound to GSTs. These *p*-substituted thiophenols provide control of

(6) (a) Xiao, G.; Liu, S.; Ji, X.; Johnson, W. W.; Chen, J.; Parsons, J. F.; Stevens, W. J.; Gilliland, G. L.; Armstrong, R. N. *Biochemistry* **1996**, *35*, 753. (b) Chen, W. J.; Graminski, G. F.; Armstrong, R. N. *Biochemistry* **1988**, *27*, 194. (c) Douglas, K. T. Reactivity of Glutathione in Model Systems for Glutathione S-Transferase and Related Enzymes. In *Glutathione Conjugation*; Seis, H., Ketterer, B., Eds.; Academic Press: New York, 1988; pp 1–41.

(7) (a) Brønsted, J. N.; Pedersen, K. Z. *Phys. Chem.* **1924**, *A108*, 185. (b) Brønsted, J. N.; Guggenheim, E. A. *J. Am. Chem. Soc.* **1927**, *49*, 2554.

(8) (a) Bruice, T. C.; Fife, T. H.; Bruno, J. J.; Brandon, N. E. *Biochemistry* **1962**, *1*, 7. (b) Jencks, W. P.; Gilchrist, M. *J. Am. Chem. Soc.* **1962**, *84*, 2910.

(9) (a) Bruice, P. Y.; Bruice, T. C.; Yagi, H.; Jerina, D. M. *J. Am. Chem. Soc.* **1976**, *98*, 2973. (b) Conlon, P. R.; Sayer, J. M. *J. Org. Chem.* **1979**, *44*, 262.

(10) (a) Zheng, Y. J.; Ornstein, R. L. *J. Am. Chem. Soc.* **1997**, *119*, 1523. (b) Zheng, Y. J.; Bruice, T. C. *J. Am. Chem. Soc.* **1997**, *119*, 3868.

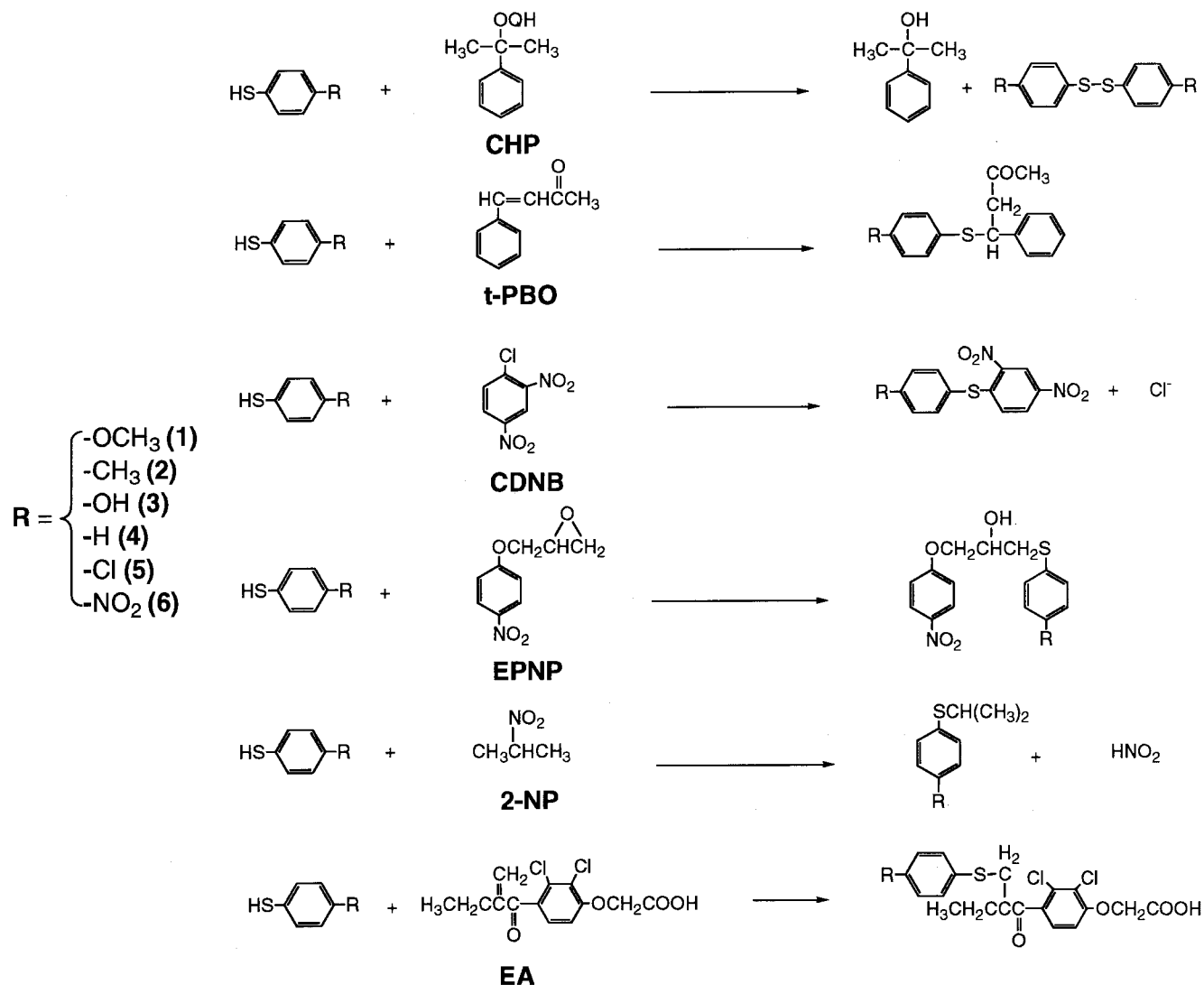


**Figure 1.** Summary of model reactions studied. The series of 4-substituted benzenethiols with variable  $pK_a$  was used in nucleophilic reactions with the indicated electrophiles, CHP, *trans*-PBO, CDNB, EPNP, and 2-NP. The R groups affording different thiol  $pK_a$  values are summarized to the left of the reactions and include *p*-methoxy (1), -methyl (2), -hydroxy (3), unsubstituted (4), -chloro (5), and -nitro (6).

the  $pK_a$  of the conjugate acid of the reactive nucleophile without complication due to differential solvation or steric effects at the nucleophilic atom. The electrophiles used represent common GST substrates and include the aryl-halide CDNB, an epoxide, a nitroalkane, a hydroperoxide, and two substrates that contain an  $\alpha,\beta$ -unsaturated carbonyl. Together, these reactions provide a quantitative analysis of the theoretical contribution of linear free energy relationships to isozyme-dependent substrate selectivity of GSTs and their pH vs rate behavior.

To link the model studies with the enzymatic system, experiments were performed with a series of GSTA1-1 mutants having variable  $pK_a$  in the [E·GSH] complex. These studies demonstrated that the linear free energy relationships described by the Brønsted relationship often will not be expressed in GST reactions at steady state due to the prevalence of rate-limiting physical steps. However, when rates of the chemical conjugation step can be observed, the intrinsic reactivity of enzyme-bound  $\text{GS}^-$  is a function of the GSH  $pK_a$ , precisely as predicted by Brønsted behavior. On the basis of these results, we suggest that the heterogeneity of the  $pK_a$  of GSH bound at the active sites of different GSTs may contribute to the 'substrate diversity' of the GST family and hence contribute to the function of these detoxication enzymes.

## Results

**Brønsted Analysis: The General Case.** For the general enzymatic reaction catalyzed by GST with any electrophile, E,  $V_{\max} = k_{\text{cat}}[\text{GST}\cdot\text{GS}^-\cdot\text{E}]$  or  $k_{\text{cat}}[\text{GST}\cdot\text{GS}\cdot\text{E}]$ , where  $k_{\text{cat}}$  is the first-order rate constant for the chemical conjugation step or diffusion-controlled product release. The analysis below relates to cases in which the chemical step is rate limiting. Assuming that the protonated complex  $[\text{GST}\cdot\text{GSH}\cdot\text{E}]$  is not catalytically competent and that the thiol and thiolate complexes are in rapid equilibrium, then for a specific pH the fraction of total GST in the active form varies with the  $pK_a$  of bound GSH. Therefore, at any pH the relative  $V_{\max}$ ,  $(V_{\max})_{\text{rel}}$ , may be defined as the fraction of the optimal rate at complete ionization of GSH,  $(V_{\max})_{\text{opt}}$ , that would be obtained if the GSH  $pK_a$  was sufficiently low, and assuming that  $k_{\text{cat}}$  is independent of the  $pK_a$ :

$$(V_{\max})_{\text{rel}} = V_{\max}/(V_{\max})_{\text{opt}} = k_{\text{cat}}[\text{GST}\cdot\text{GS}^-\cdot\text{E}]/k_{\text{cat}}\{[\text{GST}\cdot\text{GSH}\cdot\text{E}] + [\text{GST}\cdot\text{GS}^-\cdot\text{E}]\} \quad (2)$$

As the  $pK_a$  changes, perhaps through evolution or in vitro mutagenesis, then the change in  $V_{\max}$  will be readily predicted from the change in the fraction of complexed GSH in the thiolate

form,  $f$ , according to eq 3 or eq 4, where  $(V_{\max})_{\text{rel}} = (k_{\text{cat}})_f$ :

$$\text{pH} = \text{p}K_a + \log \left\{ \frac{[\text{GST} \cdot \text{GS}^- \cdot \text{E}]}{[\text{GST} \cdot \text{GSH} \cdot \text{E}]} \right\} \quad (3)$$

or

$$\text{pH} = \text{p}K_a + \log \left\{ \frac{[f]}{[1-f]} \right\} \quad (4)$$

With this simple ionization model, enzyme turnover is controlled only by the fraction of GST complexed with the thiolate  $\text{GS}^-$  at any pH and  $\text{p}K_a$ .

However, according to classic descriptions of free energy relationships, as the enzyme lowers the  $\text{p}K_a$  of GSH, the resulting  $\text{GS}^-$  becomes less reactive, according to eq 1, where  $k$  or  $k_{\text{cat}}$  is the intrinsic rate constant for the uncatalyzed or enzyme catalyzed reaction, respectively. In this case, competing effects will be operative. As evolution or mutagenesis changes the  $\text{p}K_a$  of GSH, the rate of product formation will be determined not only by the fraction of enzyme in this form but also by the  $k_{\text{cat}}$  associated with new  $\text{p}K_a$ , as determined by eq 1. If  $\beta_{\text{nuc}}$  from the Brønsted relation (eq 1) is sufficiently low, as suggested previously, then  $k_{\text{cat}}$  will be insensitive to changes in GSH  $\text{p}K_a$  and  $V_{\max}$  will depend, in the limiting case, on the fraction of GST complexed as  $[\text{GST} \cdot \text{GS}^- \cdot \text{E}]$ , as in the simple ionization model. However, if  $\beta_{\text{nuc}}$  is sufficiently large to cause changes in  $k_{\text{cat}}$  as the GSH  $\text{p}K_a$  changes, then  $V_{\max}$  becomes a complex function of  $\beta_{\text{nuc}}$ , pH, and GSH  $\text{p}K_a$ .

Because the goal of the present analysis was to explore the role of variable GSH  $\text{p}K_a$  in electrophilic substrate selectivity of GSTs rather than to provide any detailed comparison of transition state structures, the constant term  $C$  in eq 1 may be eliminated. As long as  $C$  in eq 1 is independent of  $\text{p}K_a$ , a convenient general expression for the *relative* rate of product formation,  $(V_{\max})_{\text{rel}}$ , for each electrophile as a function of the  $\text{p}K_a$  of GSH in the enzyme complex is readily obtained and accounts for the dependence of  $k_{\text{cat}}$  on  $\text{p}K_a$ . To do this, we define the parameter  $(V_{\max})_f$ , which is the rate of product formation at a GSH  $\text{p}K_a$  that affords  $(k_{\text{cat}})_f$  and fractional ionization of the GSH thiol defined above as  $f$ . Similarly, the optimal rate,  $(V_{\max})_{\text{opt}}$ , is now the  $V_{\max}$  at a  $\text{p}K_a$  that yields optimal rate by balancing  $\text{p}K_a$ -dependent  $k_{\text{cat}}$  and  $f$ . Thus, if  $(V_{\max})_f$  is normalized to  $(V_{\max})_{\text{opt}}$ , then we obtain  $(V_{\max})_{\text{rel}}$ , the fraction of optimal  $V_{\max}$  at any  $\text{p}K_a$ :

$$(V_{\max})_{\text{rel}} = (V_{\max})_f / (V_{\max})_{\text{opt}} = [(k_{\text{cat}})_f \cdot f] / [(k_{\text{cat}})_{\text{opt}}] \quad (5)$$

$$(V_{\max})_{\text{rel}} = [f] \cdot (k_{\text{cat}})_{\text{rel}} \quad (6)$$

Thus  $(V_{\max})_{\text{rel}}$  and  $(k_{\text{cat}})_{\text{rel}}$  are unitless. When the expression for  $f$  from eq 4 and the expression for  $k_{\text{cat}}$  from eq 1 are substituted into eq 6, we obtain an expression for  $(V_{\max})_{\text{rel}}$  in terms of GSH  $\text{p}K_a$ , pH, and  $\beta$ :

$$(V_{\max})_{\text{rel}} = \left\{ 10^{(\beta)(\text{p}K_a)} \cdot [10^{(\text{pH}-\text{p}K_a)}] \right\} / [1 + 10^{(\text{pH}-\text{p}K_a)}] \quad (7)$$

For convenience, the dependence of  $(V_{\max})_{\text{rel}}$  on pH,  $\text{p}K_a$ , and  $\beta$  will be referred to as the Brønsted GST model. Equation 7 was used to perform a numerical simulation (Figure 2), which illustrates several important features of the dependence of rate on  $\beta_{\text{nuc}}$  and  $\text{p}K_a$ . In Figure 2, the rates have been determined for pH 8.0, 7.4, and 6.5 and normalized in each case to the maximal value obtained for each  $\beta_{\text{nuc}}$  value,  $(V_{\max})_{\text{opt}}$ . The normalized rates,  $(V_{\max})_{\text{rel}}$ , provide a measure of the sensitivity of the rate of turnover for each electrophile as the thiol  $\text{p}K_a$  changes. For each value of  $\beta_{\text{nuc}}$  and at any specific pH, there

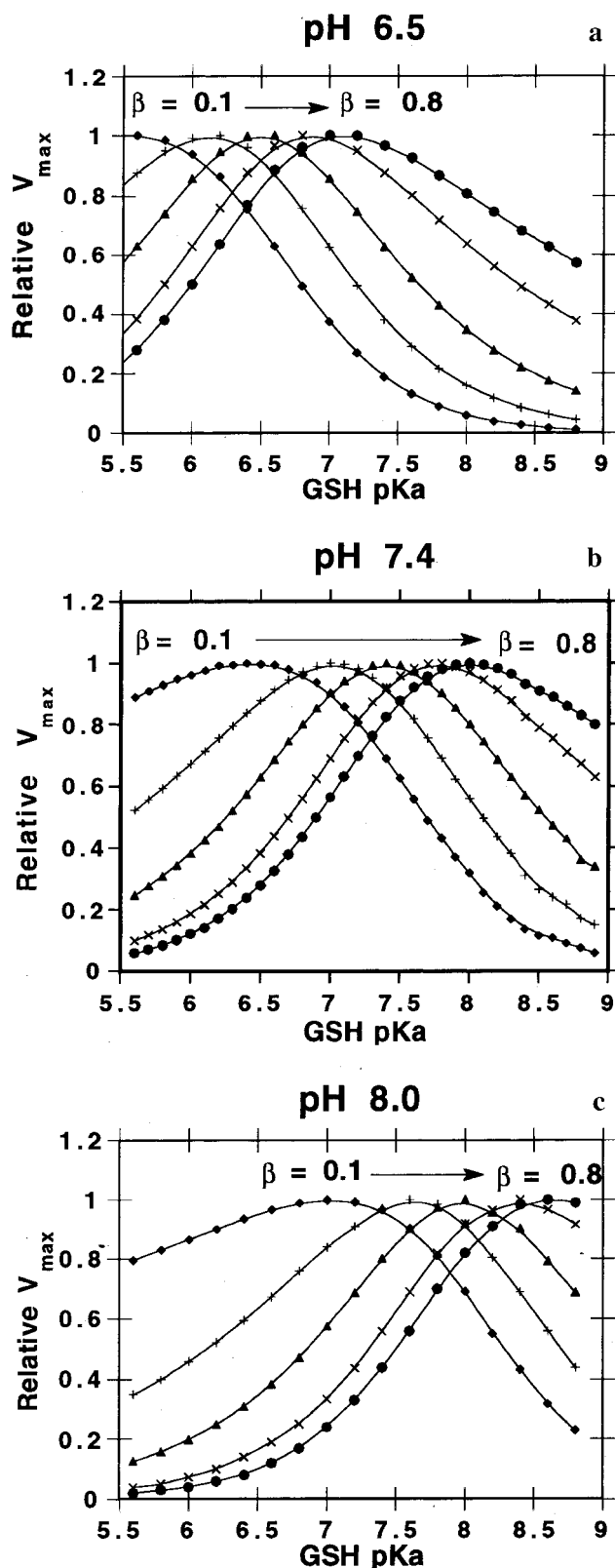


**Figure 2.** Plots of relative  $V_{\max}$  vs GSH  $\text{p}K_a$  at variable  $\beta_{\text{nuc}}$ , as predicted by eq 7. As  $\beta_{\text{nuc}}$  increases from 0.1 to 0.9, the  $\text{p}K_a$  optimum for the reaction increases. The precise optimum is also a function of pH. The  $\beta_{\text{nuc}}$  for the symbols used are  $\blacklozenge$ , 0.1;  $+$ , 0.3;  $\blacktriangle$ , 0.5;  $\times$ , 0.7;  $\bullet$ , 0.8. (a) pH 6.5, (b) pH 7.4, (c) pH 8.0.

is an optimal  $\text{p}K_a$  for GSH bound at the active site of GST. If the  $\text{p}K_a$  is below this optimum, then the decrease in intrinsic reactivity associated with Brønsted-type linear free energy relation 'outweighs' the gain in  $f$  that results from lowering the



$pK_a$ . Also, the steepness of the  $pK_a$  vs rate profile is greater on the high  $pK_a$  side for low  $\beta_{nuc}$  values. However, as  $\beta_{nuc}$  approaches 1 the curves become less steep on the high  $pK_a$  side and more sensitive on the low  $pK_a$  side. Note that, because each curve is normalized within the data for a given electrophile, comparison of rates for different electrophiles at a specific  $pK_a$  is not informative. However, the results emphasize that, according to Brønsted model, the dependence of the reaction rates on GSH  $pK_a$  differs dramatically with the  $\beta_{nuc}$  values and with pH.

#### Determination of Brønsted Factors in Chemical Models.

To compare the effect of variable GSH  $pK_a$  on the rate of reaction with different electrophiles, it was necessary to determine  $\beta_{nuc}$  values for a representative range of electrophilic substrates of GSTs. That is, the relevance of Figure 2 for GST catalysis is unclear in the absence of  $\beta_{nuc}$  values for electrophilic GST substrates. Furthermore, because the dielectric environment of GST active sites is uncharacterized, it was necessary to explore the effect of solvent hydrophobicity on  $\beta_{nuc}$  values. Therefore, the rate constants for the reactions of a series of thiols with different  $pK_a$  values with several electrophiles (Figure 1) were determined under different solvent conditions. For each thiol–electrophile conjugate, the rate of product formation was determined spectrophotometrically by measuring loss of chromophoric thiol reactant, as described in the Experimental Section. To validate this method for determination of rate constants and to ensure that thiol oxidation was not contributing to the thiol consumption, the rate constants for reactions were determined also by monitoring product formation for the series of thiols with the electrophile CDNB. CDNB is a ‘universal’ GST substrate, and CDNB conjugates are easily quantitated by colorimetric assay. Thus, synthetic standards were prepared for each thiol–CDNB conjugate, and the extinction coefficients were determined (Experimental Section) to ensure precise measurement of rate constants. The rate constants and  $\beta_{nuc}$  value obtained for this series of reactions were identical whether determined by following loss of thiol or by production of CDNB conjugate. Thus, the former method is assumed to yield accurate  $\beta_{nuc}$  values with the other electrophiles, without contribution from thiol oxidation. Typical raw progress curves are shown in Figure 3, which demonstrates the expected concentration dependence on rate of thiol consumption. The Brønsted plots for a subset of electrophiles and the series of thiols also are summarized in Figure 3. The recovered Brønsted values for each electrophile are summarized in Table 1. Reaction with each electrophile shown in Figure 1 was studied in 10% DMF. Additional reactions were run in 30% DMF. There has been significant debate concerning the relevant dielectric constants for enzyme active sites, and it is not the goal of these studies to accurately model the dielectric environment of GST active sites. Rather, the experiments are intended to emphasize that  $\beta_{nuc}$  values are almost certainly greater for active site processes than in aqueous solution for many electrophiles. As expected on the basis of previous studies of thiol attack on electrophilic centers,  $\beta_{nuc}$  values increase with increasing hydrophobicity of the solvent.

In cases where direct comparison is possible, the recovered values are in good agreement with  $\beta_{nuc}$  values reported for thiol attack on various electrophiles.<sup>6c,9</sup> We do note that, for CDNB and EPNP, the values obtained here are modestly higher than reported reactions with aliphatic thiols; this is likely a result of using arylthiols rather than alkanethiols and from inclusion of the hydrophobic solvent as observed for other electrophiles (and *vide infra*). Also, it should be noted that thiolate reactions with

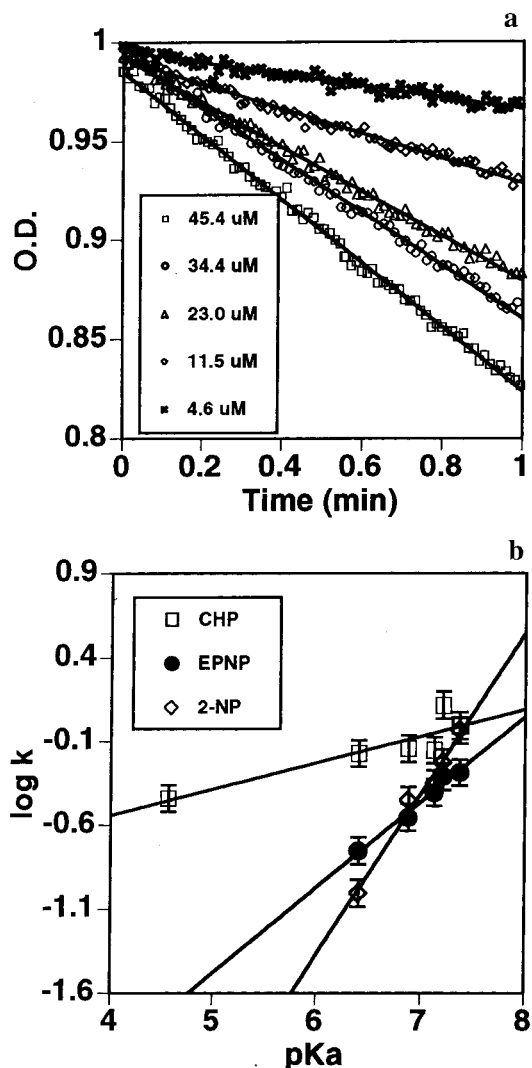


**Figure 3.** (a) Raw progress curves for reaction of thiobenzene (**4**) with CDNB. The effect of varying the concentration of thiol on the rate is shown. The offset in absorbance values at time 0 is due to different extents of reaction occurring before initiating measurements. The slopes (fitted lines) yield  $k_{obs}$  at each concentration. See methods for details. (b) Representative Brønsted plots for various electrophiles. Both  $C$  and  $\beta_{nuc}$  of eq 1 vary with electrophile. The full range of  $\beta_{nuc}$  values are summarized in Table 1.

**Table 1.** Brønsted Coefficients for Electrophilic GST Substrates<sup>a</sup>

electrophile	$\beta_{nuc}$	
	90:10, H <sub>2</sub> O:DMF	70:30, H <sub>2</sub> O:DMF
CHP	0.16 ± 0.04	0.29 ± 0.04
CDNB	0.46 ± 0.08	0.66 ± 0.01
EPNP	0.51 ± 0.08	0.63 ± 0.05
EA	0.59 ± 0.01	
<i>trans</i> -PBO	0.78 ± 0.10	
2-NP	0.93 ± 0.08	1.04 ± 0.13
range	$\Delta\beta_{nuc} = 0.77$	$\Delta\beta_{nuc} > 0.68$

<sup>a</sup> See Experimental Section for reaction conditions. Plots used to determine  $\beta_{nuc}$  values were obtained with triplicate kinetic runs. Typical progress curves are shown in Figure 3a, and representative Brønsted plots are shown in Figure 3b. For all electrophiles other than CHP and *t*-PBO, regression analysis of the Brønsted plots yielded  $r^2 > 0.95$ . For CHP and *t*-PBO,  $r^2$  values were 0.90 and 0.91, respectively.

unbranched nitroalkanes proceed via a  $S_N2$  nucleophilic mechanism, whereas  $\alpha$ -substituted nitroalkanes may proceed by a radical-anion chain mechanism,  $S_{RN}1$  mechanism.<sup>11,12</sup> Indeed, multiple mechanisms may be operative with GST catalysis.

Obviously, our results are relevant only for nitroalkanes that react via a nucleophilic,  $S_N2$  mechanism.

**Application of the Model to GST-Dependent Reactions.** In light of the model studies that indicate the  $\Delta\beta_{\text{nuc}}$  range is large enough to contribute to electrophile-dependent differences in  $V_{\text{max}}$ , it is of interest to determine their predictive value in relation to the enzyme-catalyzed reactions. For example, the Brønsted analysis suggests that a GST complexed with GSH having  $\text{p}K_{\text{a}}$  of 8 should be more reactive with electrophiles characterized by large  $\beta_{\text{nuc}}$  values than a GST with a cofactor  $\text{p}K_{\text{a}}$  of 6.5. In contrast, reactions characterized by low  $\beta_{\text{nuc}}$  values should be more efficiently catalyzed by GSTs that afford a GSH  $\text{p}K_{\text{a}}$  of 6.5 than 8. Moreover, at higher pH the rate of reaction with a low  $\beta_{\text{nuc}}$  value will be a more sensitive function of the  $\text{p}K_{\text{a}}$  of GSH than at low pH. The extent to which these predictions are observable depends on whether the experimentally monitored kinetic parameter reflects the microscopic rate constant for the chemical conjugation step. If the chemical step for enzymatic turnover is not rate limiting, then the free energy relationship will be masked in steady-state experiments.

To determine whether chemical steps are rate limiting for enzymatic turnover of the electrophiles used in the model studies, enzymatic reactions were performed in the presence of varying concentrations of viscogen. When physical steps such as ligand association or dissociation are rate limiting, the overall turnover rate decreases with increasing viscogen. In contrast, if chemical steps are rate limiting, the steady-state rate is insensitive to viscogen. The use of viscogens as probes of segmental motion has been described for several enzymatic systems including GSTs.<sup>13</sup> No turnover was detected with *t*-PBO or EPNP with this particular GST isozyme, and an enzymatic assay for 2-NP turnover is not readily available. The influence of viscogen on reaction rates for wild-type GSTA1-1, at pH 7.4, with CHP, CDNB, and EA is shown in Figure 4 (a). These results clearly demonstrate that chemical conjugation is cleanly rate limiting only for CHP ( $m = 0.01$ ). Physical steps are cleanly rate limiting for EA ( $m = 0.92$ ). Intermediate slopes for plots of this type ( $m = 0.12$ ), as with CDNB, may reflect a partially rate-limiting chemical step. Therefore, CHP and CDNB were used as substrates with a series of mutants, previously described, including F220Y, F220E, F220I, and F220L.<sup>4c,14</sup> These mutants are catalytically comparable to the wild type but exhibit variable  $\text{p}K_{\text{a}}$  for the [GST•GSH] complex. Importantly, Phe-220 does not directly contact the electrophile binding site nor the sulfur atom of the  $\text{GS}^-$  nucleophile but rather provides part of the immediate environment of the catalytic Tyr-9, which in turn modulates the  $\text{p}K_{\text{a}}$  of GSH at the active site via an indirect effect. Together with wild type, these mutants provide a limited set of GSTs with variable GSH  $\text{p}K_{\text{a}}$  ( $\text{p}K_{\text{a}}$  7.0–9.0), with minimal structural variation expected in the immediate environment of the  $\text{GS}^-$  thiolate or the electrophile. Chemical steps are cleanly rate limiting for each GST variant when CHP is the substrate (Figure 4b,  $m = 0.007$ – $0.059$ ), but physical steps contribute differentially with these variants when CDNB is the substrate, as indicated by the slopes

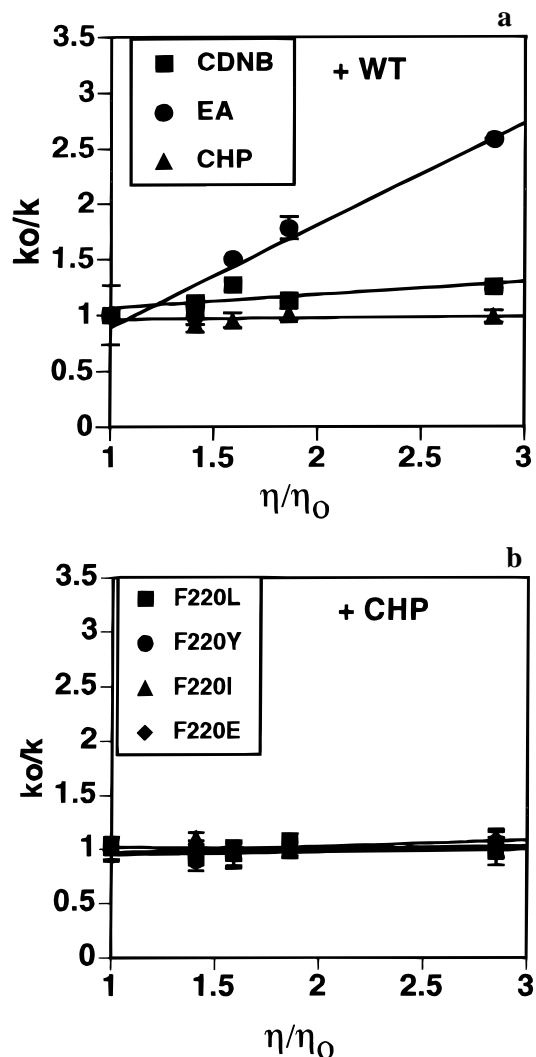


**Figure 4.** Dependence of steady-state turnover rates on viscogen at pH 7.4. (a) Rates of enzymatic reaction vs viscogen concentration are shown for wild-type rat GSTA1-1 with CHP, CDNB, and EA. Only the reaction with CHP is limited cleanly by chemical steps. (b) Rates of reaction vs viscogen concentration for CHP and mutant GSTs with variable GSH  $\text{p}K_{\text{a}}$ . Mutation-induced changes in  $\text{p}K_{\text{a}}$  do not change the rate-limiting step for this substrate. For each data set, the fitted lines were obtained from  $k_0/k = n/n_0$  where  $k_0$  and  $k$  are the rates in the absence and presence of viscogen and  $n_0$  and  $n$  are the viscosities. The slopes obtained with EA, CDNB, and CHP are 0.92, 0.12, and 0.012, respectively (a). The slopes obtained for CHP remained  $<0.05$  for each of the mutants (b).

ranging from 0.062 to 0.34 (not shown). Thus, Brønsted behavior will likely be masked partially in steady-state experiments with CDNB. On the basis of these results, experimental challenge of the model defined by eq 7 with steady-state  $V_{\text{max}}$  rates (or  $k_{\text{cat}}/K_{\text{M}}$ ) for the EA substrate is not possible and will require more detailed pre-steady-state kinetic analysis that yields microscopic rate constants for chemical conjugation steps.

Brønsted analysis was performed for enzymatic turnover of CDNB and CHP, at three pHs. The  $\beta_{\text{nuc}}$  values for the enzymatic turnover of CHP and CDNB were determined from plots of  $(V_{\text{max}})_{\text{lim}}$  vs GSH  $\text{p}K_{\text{a}}$ , where  $(V_{\text{max}})_{\text{lim}}$  is the limiting rate at high pH, where all of the complexed GSH is ionized. This method has been previously described,<sup>4f,6b</sup> and the Brønsted plots are shown in Figure 5. Notably, the recovered  $\beta_{\text{nuc}}$  value for the enzymatic reaction with CHP,  $0.19 \pm 0.08$ , is in excellent agreement with the values obtained in the model systems. The recovered value for CDNB,  $0.25 \pm 0.07$ , is in reasonable

(11) Benn, M.; Meesteres, A. C. *J. Am. Chem. Soc. Chem. Commun.* **1977**, 597.

(12) (a) Bowman, W. R. *Chem. Soc. Rev.* **1988**, 17, 283. (b) Bowman, W.; Richardson, G. *Tetrahedron Lett.* **1981**, 22, 1551.

(13) (a) Caccuri, A. M.; Antonini, G.; Nicotra, M.; Battistoni, A.; Lo Bello, M.; Board, P. G.; Parker, M. W.; Ricci, G. *J. Biol. Chem.* **1997**, 272, 2968. (b) Johnson, W. W.; Liu, S.; Ji, X.; Gilliland, G. L.; Armstrong, R. N. *J. Biol. Chem.* **1993**, 268, 11508. (c) Sampson, N.; Knowles, J. *Biochemistry* **1992**, 31, 8488. (d) Adams, J.; Taylor, S. S. *Biochemistry* **1992**, 31, 8516.

(14) Atkins, W. M.; Dietze, E. C.; Ibarra, C. *Protein Sci.* **1997**, 6, 873.

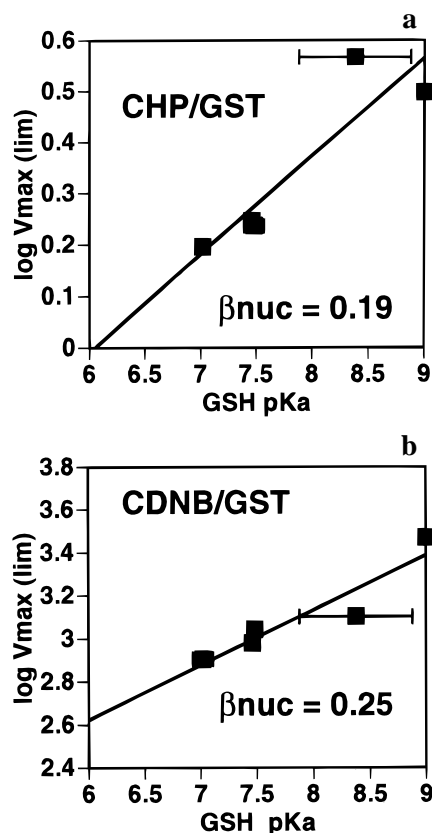


**Figure 5.** Brønsted plots for enzymatic turnover with CHP and CDNB.  $(V_{\max})_{\text{lim}}$  at complete GSH ionization was determined from plots of  $\log V_{\max}$  vs pH for each mutant. The resulting plots were fit to the equation  $\log V_{\max} = \log\{(V_{\max})_{\text{lim}}/[1 + [H^+]/K_a]\}$ , where  $K_a$  is the acid ionization constant of GSH bound to each GST. Values of  $(V_{\max})_{\text{lim}}$  recovered from these analyses for each protein are plotted vs the  $pK_a$  of complexed GSH to obtain  $C$  (y-intercept) and  $\beta_{\text{nuc}}$  (slope). The recovered values are  $C = -1.16$  and  $\beta_{\text{nuc}} = 0.19 \pm 0.08$  for CHP;  $C = 2.61$  and  $\beta_{\text{nuc}} = 0.25 \pm 0.14$  for CDNB.

agreement with the model studies, although slightly lower. Presumably, the contribution of diffusion-limited processes to the rate-limiting step with CDNB (Figure 4) contributes to masking of the true  $\beta_{\text{nuc}}$  value, and CDNB is likely to fit the steady-state Brønsted model less well than CHP.

Further analysis with CHP was performed in order to determine whether the linear free energy relationship predicted by eq 7 was operative. The experimentally determined  $\beta_{\text{nuc}}$  and  $C$  values for CHP (Figure 5) were used with eq 1 to calculate the  $V_{\max}$  rate at the optimal  $pK_a$ . This calculated rate,  $(V_{\max})_{\text{opt}}$ , was used to calculate  $(V_{\max})_{\text{rel}}$  from eq 2 and the experimentally measured rates of  $V_{\max}$  for CHP with each protein at each of the three pHs. Simulated curves of  $(V_{\max})_{\text{rel}}$  vs GSH  $pK_a$ , at three pHs, were constructed according to the simple ionization model (eq 2), and the Brønsted model, (eq 8) using the experimentally determined  $\beta_{\text{nuc}}$  and  $C$  values for enzymatic turnover of CHP. Equation 8 is derived with the same strategy as eq 7 was derived, except the constant term  $C$  in eq 1 is retained. This is required because absolute rates and not normalized rates are experimentally obtained:

$$(V_{\max})_{\text{rel}} = \{10^{(\beta)(pK_a)} \cdot [10^{(pH-pK_a)}]\} / [1 + 10^{(pH-pK_a)}] + [10^C \cdot 10^{(pH-pK_a)}] / [1 + 10^{(pH-pK_a)}] \quad (8)$$

The simulated curves for the ionization model are shown as dashed lines in Figure 6, and the simulated Brønsted models are shown with a solid line. The calculated relative rates

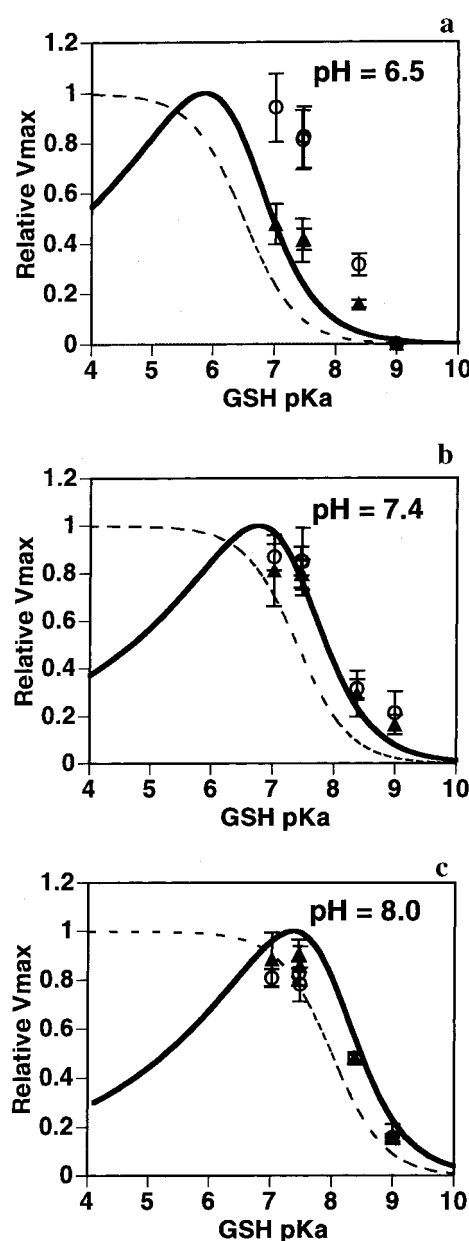


**Figure 6.** Comparison of the simple ionization model and the Brønsted model. The experimentally determined  $(V_{\max})_{\text{rel}}$  values (▲) are plotted for the mutants with variable GSH  $pK_a$ . The  $(V_{\max})_{\text{rel}}$  values are obtained from normalization to  $(V_{\max})_{\text{opt}}$  for the Brønsted model. The solid lines represent the fitted curves according to the Brønsted GST model, in which  $k_{\text{cat}}$  varies with  $pK_a$ , as described by eq 7 in the Results. Open circles are experimentally determined  $(V_{\max})_{\text{rel}}$  values using the  $(V_{\max})_{\text{opt}}$  from eq 2 or the simple ionization model. The dashed line represents the fitted curves for the simple ionization model, in which  $k_{\text{cat}}$  is insensitive to changes in  $pK_a$ . Even for electrophiles with low  $\beta_{\text{nuc}}$  values, the experimental rates are perturbed from the simple ionization model as predicted by the Brønsted GST model.

obtained from the experimentally measured absolute rates also are shown in Figure 6, normalized to  $(V_{\max})_{\text{opt}}$  as predicted by either the simple ionization model (open circles) or the Brønsted model (closed triangles). Excellent agreement was observed between the experimentally determined rates for the GST variants and the model that incorporates Brønsted free energy linkage. Indeed, statistical fitting of the two models, ionization only, according to eq 2, vs eq 7, indicates that the experimental data fit better when Brønsted behavior is included, particularly at the lower pHs. The  $\chi^2$  values for pH 6.5, pH 7.4, and pH



8.0 are 0.074, 0.037, and 0.043, respectively, when the data are fit to the Brønsted model; the corresponding  $\chi^2$  values are 1.63, 0.41, and 0.050 when fit to the simple ionization model.

## Discussion

Linear free energy relationships have been analyzed for a series of thiol acids with variable  $pK_a$  and the nucleophilic reaction of their conjugate bases with a range of electrophiles. The thiol acids of both small molecule models and GSH complexed to GST variants have been studied experimentally. Although linear free energy relationships, including Brønsted analysis, have been utilized extensively in attempts to delineate transition-state structure for enzyme-catalyzed reactions,<sup>15</sup> the goal of the experiments described here was significantly different; the present model studies provide a basis for predicting quantitatively the change in apparent rate of reaction for conjugation of the nucleophilic  $GS^-$  with several electrophilic GST substrates, as a function of the  $pK_a$  of the enzyme-bound GSH. Because the  $pK_a$  of GSH at the active site of different GST isozymes (wild type) varies by as much as  $\sim 1$   $pK_a$  unit, these models were developed in order to determine whether the observed differences in GST isozyme selectivity for different electrophiles are due partially to differences in intrinsic reactivity of the individual  $[GST \cdot GS^- \cdot E]$  complexes. We are cautious to not over interpret the  $\beta_{nuc}$  values for these model systems in terms of detailed transition-state structures of the enzyme-catalyzed reaction. Indeed, it is reasonable to question the utility of  $\beta_{nuc}$  values determined here for small molecule model systems in understanding the extent of bond formation or charge dispersion in the enzyme-catalyzed reactions. The question of whether enzymes can control parameters that determine slopes of plots derived from linear free energy relationships has been discussed, and it is possible that  $\beta_{nuc}$  values are 'tuned' by enzymes.<sup>16</sup> Solvent dramatically affects  $\beta_{nuc}$  values, and enzyme active sites provide 'solvation' different from bulk aqueous phase. Presumably, then,  $\beta_{nuc}$  values will differ for the two environments (see below). However, it is unlikely that, for a wide range of electrophiles, the  $\beta_{nuc}$  values determined in bulk solution would converge to a single value or narrow range of values for active site processes. Importantly, some compression of  $\beta_{nuc}$  values is expected with increasing solvent hydrophobicity because the theoretical upper limit is 1.0. With increasing solvent hydrophobicity, therefore, the range of  $\beta_{nuc}$  values may become smaller, but their average magnitude will become larger (Table 1). As emphasized above, the actual  $\beta_{nuc}$  values are not used here to interpret details of the enzymatic reaction mechanisms, and these values are likely to be crude approximations given the unknown dielectric constant of the GST active site and the use of aryl thiols. Rather, the model studies are intended to demonstrate that  $\beta_{nuc}$  values are *not universally low* for all thiol-electrophile pairs, as suggested previously. Regardless of the actual values, the studies presented here indicate the likelihood of a wide range of  $\beta_{nuc}$  for GST-catalyzed conjugation of GSH with different electrophiles.

Most importantly, the major conclusion obtained from these model studies is that a difference of  $\sim 1$   $pK_a$  unit, as reported for GSH bound to a GST M3-3 vs GST A1-1, should afford a significant difference in  $k_{cat}$  as the electrophile changes, such that  $V_{max}$  will change in accord with eq 7, and not be a simple

function of the fraction of ionization of GSH. The significance of this conclusion is most apparent with a specific, theoretical, example based in Figure 2. Figure 2 predicts that, for a reaction with  $\beta_{nuc}$  value of  $\sim 0.1$  at pH 7.4, the ratio of  $V_{max}$  rates for a GST complex with  $pK_a$  of 6.5 to a complex with  $pK_a$  7.5 ( $V_{max,6.5}/V_{max,7.5}$ ) will be 1.9, and there is a catalytic advantage for the isozyme with the lower  $pK_a$ . In contrast, the analogous ratio for a reaction with a  $\beta_{nuc}$  value of 0.8 will be 0.25. In this case, the complex having the higher  $pK_a$  will exhibit the faster turnover for the Michael-type addition. Thus, there is a 7.7-fold difference in the selectivity of the two isozymes for the electrophile with a low  $\beta_{nuc}$  value relative to the ratio of their selectivities for the substrate characterized by the high  $\beta_{nuc}$ . Also, depending on the electrophilic substrate, there will be different optimal GSH  $pK_a$  values that balance the increased fraction of thiolate with the decreased nucleophilicity of the resulting thiolate, and this optimal  $pK_a$  will vary with solution pH. Therefore, the results summarized in Figure 2 indicate that the relative substrate selectivity for GST isozymes with different GSH  $pK_a$  values may be partially controlled by the linear free energy relationship described in 'traditional' Brønsted analysis. The extent to which these proposals are relevant to GST catalysis depends on the range of  $\beta_{nuc}$  values spanned by reactions with different GST electrophilic substrates. The model studies indicate that this range is large, with  $\Delta\beta_{nuc}$  as large as 0.5–0.6, conservatively, depending on the hydrophobicity of the reaction environment. Therefore, differences in GSH  $pK_a$  associated with different isozymes or due to mutagenic variation are likely to cause modest differences in the inherent nucleophilicity of the  $GS^-$  nucleophile at their active sites.

There are several mechanisms by which the linear free energy relationships may be masked in enzymatic reactions. Obviously, active site architecture, or topology, also contributes to isozyme-dependent substrate selectivity. Numerous examples of amino acid substitutions that lead to altered substrate selectivity of GSTs, including stereochemical selectivity, have been reported.<sup>17</sup> Furthermore, differences in substrate selectivity can be intuitively rationalized in some cases by comparing the available X-ray structures. Certainly, comparison of turnover rates for a specific electrophile between GSTs with different GSH  $pK_a$  values will be complicated by differences in active site topology, which are likely to dominate the isozyme-dependent substrate selectivity profile.

A second determinant of isozyme-dependent substrate selectivity, especially across class boundaries, results from the presence of additional catalytic elements present in some, but not all, GSTs. For example, M class GSTs have been shown to utilize general acid catalysis via an active site tyrosine distinct from the GSH hydrogen bond partner to the leaving oxygen during epoxide conjugation.<sup>13b</sup> Obviously, even if chemical steps do control  $V_{max}$  in such cases, the additional catalytic groups present in some isozymes will increase the apparent, intrinsic, nucleophilicity of the  $GS^-$  anion, and a comparison of rates with isozymes from other classes that do not have a similar acid catalyst is futile. Together, the differences in active site topology and catalytic groups makes difficult a comparison of the GSH  $pK_a$  and substrate selectivity for GSTs belonging to different classes. In contrast, our model studies have eliminated these effects by design, and the analysis provided here indicates that if other active site features are identical, then the  $pK_a$  of enzyme-bound GSH will be an important determinant of the substrate selectivity of GST isozymes. This conclusion

(15) (a) Toney, M. D.; Kirsch, J. F. *Science* **1989**, *243*, 1485. (b) Schweins, T.; Geyer, M.; Kalbitzer, H. R.; Wittinghofer, A.; Warshel, A. *Biochemistry* **1996**, *35*, 14225.

(16) (a) Burbaum, J. J.; Raines, R. T.; Albery, W. J.; Knowles, J. R. *Biochemistry* **1989**, *28*, 9293. (b) Ellington, A. D.; Benner, S. A. *J. Theor. Biol.* **1987**, *127*, 491.

(17) (a) Bammler, T.; Driessen, H.; Finnstrom, N.; Wolf, C. R. *Biochemistry* **1995**, *34*, 9000. (b) Zhang, P.; Liu, S.; Shan, S.; Ji, X.; Gilliland, G. L.; Armstrong, R. N. *Biochemistry* **1992**, *31*, 10185.



is based in Figure 2, which highlights the dependence of rate on  $\beta_{\text{nuc}}$  and GSH  $\text{p}K_{\text{a}}$ , and Table 1, which demonstrates that  $\Delta\beta_{\text{nuc}}$  is likely to be large enough to contribute to rate differences for some electrophiles.

The enzymatic experiments clearly indicate a third source of deviation from the Brønsted GST model. The studies with variable concentration of viscogen provide an essential reminder that the contribution of linear free energy relationships to substrate selectivity of GSTs with variable  $\text{p}K_{\text{a}}$  will be masked if only steady-state kinetic parameters are compared. For many electrophile•GST pairs, physical steps are rate limiting. Therefore,  $V_{\text{max}}$  and its pH dependence will not exhibit the variation with GSH  $\text{p}K_{\text{a}}$  predicted by the Brønsted analysis. The linear free energy relationships will only be expressed fully for a subset of [GST•GS<sup>-</sup>•electrophile] combinations, such as the [GSTA1-1•GS<sup>-</sup>•CHP] complex. Indeed, the results obtained for enzymatic turnover of CHP, summarized in Figure 6, demonstrate a remarkable adherence to the pH and GSH  $\text{p}K_{\text{a}}$  dependence that is predicted by eq 7. Together the results demonstrate that the  $\text{p}K_{\text{a}}$  of GSH at the active site of GSTs plays a modest role in the electrophile-dependent efficiency of chemical steps in the reaction cycle.

The  $\beta_{\text{nuc}}$  values obtained for GST-dependent turnover of CHP and CDNB warrant some discussion.  $\beta_{\text{nuc}}$  has been determined to be  $0.3 \pm 0.2$  for GSH conjugation to CDNB by an M class GST.<sup>4f,6b</sup> The A1-1 GST yields an identical value within experimental error of  $0.25 \pm 0.07$ . To whatever extent these values are interpretable at the molecular level, the mechanisms and transition states for this reaction catalyzed by the two isozymes are apparently nearly identical. The value obtained in our model studies, at 10%DMF:90%H<sub>2</sub>O, agrees reasonably well this value. Presumably, the larger value obtained in the model studies results from the use of aryl rather than alkyl thiols and the masking of the linear free energy relationship (vide infra). In contrast, the  $\beta_{\text{nuc}}$  value obtained from the model studies for CHP is nearly identical to the enzymatic result. Notably, this is only the second substrate for which the  $\beta_{\text{nuc}}$  value has been measured for a GST-dependent reaction. Together, these results suggest that the CHP reaction is characterized by a lower  $\beta_{\text{nuc}}$  value than the CDNB reaction, both in solution and enzymatically. It appears that GST active sites do not tune  $\beta_{\text{nuc}}$  values significantly far from the solution behavior as long as purely aqueous conditions are not used as a reference.

Linear free energy relationships arise when  $\Delta\Delta G$  for a series of reference equilibria, such as ionization of GSH, is partially or completely incorporated in  $\Delta\Delta G^\ddagger$  for a series of reactions involving components of the equilibria, where  $\beta_{\text{nuc}}$  is proportional to  $\Delta\Delta G^\ddagger/\Delta\Delta G$ . Here, when  $\beta_{\text{nuc}}$  is 1.0, any free energy of destabilization of the GS<sup>-</sup> anion for the variant GSTs would be expected to destabilize the ground-state anion relative to the transition state for nucleophilic attack of the thiolate by the same differential energy, i.e.,  $\Delta\Delta G = \Delta\Delta G^\ddagger$ , and the nucleophilic reactions will be slower. In as much as the transition state is 'unaffected' by the changes that perturb  $\Delta\Delta G$ , large  $\beta_{\text{nuc}}$  values are interpreted to indicate a late transition state that is very different from the starting thiolate/electrophile complex. In contrast, a low  $\beta_{\text{nuc}}$  value is observed if the stabilization of thiolate relative to thiol,  $\Delta\Delta G$ , is also apparent in stabilization of the transition state for reaction of the thiolate, such that  $\Delta\Delta G^\ddagger < \Delta\Delta G$ . These data indicate that GST-dependent metabolism of CHP and CDNB proceed through early transition states, as in the nonenzymatic reactions. The model studies suggest, however, that a late transition state is operative with other GST

substrates. Whether this is the case in the enzymatic reactions remains to be determined.

An experimental challenge of the Brønsted model, provided by CHP (Figure 6), clearly demonstrates that this model more accurately describes the reactivity of GSTs than the simple ionization model. Unfortunately, the only substrate we examined for which chemical steps are cleanly rate limiting, CHP, is also characterized by a very low  $\beta_{\text{nuc}}$  value. Obviously, a more dramatic distinction between the two models would be obtained with reactions characterized by higher  $\beta_{\text{nuc}}$  values or at lower  $\text{p}K_{\text{a}}$  ranges. Neither case is readily attainable with the available GST mutants and electrophiles surveyed here.

Although the contribution of the Brønsted free energy relationships to substrate specificity is modest, the demonstration that the  $\text{p}K_{\text{a}}$  of GSH at the active sites of GSTs contributes to rates of chemical steps naturally leads to several questions. Why has nature varied the  $\text{p}K_{\text{a}}$  among different GST isozymes? Have different GSTs evolved to optimal GSH  $\text{p}K_{\text{a}}$  values for different electrophiles? Perhaps, it is useful to contrast the role of free energy relationships for the detoxication catalysts, GSTs, with the serine proteases, which also are considered to be 'broad specificity' enzymes. The  $\text{p}K_{\text{a}}$  of the nucleophilic serine in the proteases is subject to the same 'paradox' described here for GSTs. However, a critical difference between these catalysts lies in their respective biological niches. Whereas the serine proteases collectively hydrolyze peptides with remarkably different sequence specificity, the local transition-state structures and  $\beta_{\text{nuc}}$  values will be nearly invariant for different peptide/isozyme combinations. The relatively constant  $\beta_{\text{nuc}}$  values are expected because, regardless of the substrate peptide sequence, an identical amide functional group is attacked by the serine. The amino acid side chains of the substrate peptide that dictate isozyme selectivity are remote from the reaction center, resulting in nearly identical local transition states for all substrates. In contrast, the electrophilic substrates for GST catalysis represent a wide range of functional groups, which lead to dramatically different transition states and  $\beta_{\text{nuc}}$  values, each with an optimal  $\text{p}K_{\text{a}}$  for the GSH cofactor. In fact, it may be speculated that a distribution of  $\text{p}K_{\text{a}}$  values among different GST isozymes provides a means for extending their collective substrate diversity, by optimizing some GSTs for reactions characterized by  $\beta_{\text{nuc}}$  values in the range 0.3–0.4 and optimizing others for reactions with  $\beta_{\text{nuc}}$  values in the range of 0.5–0.6. The classic linear free energy profile analysis used here reveals a simple but novel mechanism by which substrate diversity may be optimized within a family of detoxication enzymes.

## Experimental Section

**Materials and Characterization.** Each of the *p*-substituted thiophenols and electrophiles, other than CDNB, shown in Figure 1 were purchased from Aldrich Chemical (Milwaukee, WI) and were used without further purification. CDNB was purchased from Sigma Chemical (St. Louis, MO). UV/vis absorbance spectra were recorded on a Cary 3E UV/vis spectrophotometer. <sup>1</sup>H NMR spectra were obtained at 300 MHz using a Varian VXR 300 spectrometer. Low resolution FAB and EI mass spectra were obtained using a micromass 70SEQ tandem hybrid mass spectrometer.

**Reaction Kinetics.** Reactions were performed at 25 °C in 10 mM MES buffer, pH 6.7, and 10% DMF, 2 mM EDTA, 0.2 mM NiSO<sub>4</sub> to prevent oxidation of thiols. This solvent system has been established to afford negligible general acid–base catalysis for nucleophilic reactions involving thiolate anions.<sup>18</sup> Electrophile and thiol stock solutions were prepared fresh every 4 h in EtOH and DMF, respectively,

(18) (a) Capozzi, G.; Modena, G. *The Chemistry of the Thiol Group*; Patai, S., Ed.; Wiley: London, 1974; pp 785–833.

and stored under argon. To initiate reactions, 10  $\mu\text{L}$  each of thiol and electrophile was added to 680–880  $\mu\text{L}$  of buffer and 100–300  $\mu\text{L}$  of DMF under pseudo-first-order conditions with excess electrophile. Electrophile concentrations were 333  $\mu\text{M}$  EPNP, 200  $\mu\text{M}$  CDNB, 200  $\mu\text{M}$  2-NP, 200  $\mu\text{M}$  CHP, and 100  $\mu\text{M}$  *trans*-PBO, and thiol concentration was varied. For reactions with each electrophile, thiol consumption was monitored at the following wavelengths where the numbers refer to the different thiols as depicted in Figure 1: (1),  $\epsilon_{264} = 34\,900\text{ M}^{-1}\text{ cm}^{-1}$ ; (2),  $\epsilon_{265} = 18\,900\text{ M}^{-1}\text{ cm}^{-1}$ ; (3),  $\epsilon_{262} = 13\,900\text{ M}^{-1}\text{ cm}^{-1}$ ; (4)  $\epsilon_{265} = 22\,900\text{ M}^{-1}\text{ cm}^{-1}$ ; (5),  $\epsilon_{274} = 19\,800\text{ M}^{-1}\text{ cm}^{-1}$ ; (6),  $\epsilon_{416} = 13\,300\text{ M}^{-1}\text{ cm}^{-1}$ . For all reactions, the pH of the final solution was measured and used to calculate the final concentration of nucleophile, adjusted for the fraction of thiolate based on the experimentally determined  $\text{pK}_a$  values (below) and the standard Henderson–Hasselbach equation. Because the formation of CDNB–thiol conjugates is routinely quantitated by monitoring product formation rather than thiol consumption, the thiol/CDNB reaction was also performed using the thiol as excess reagent and monitoring formation of the thiol–CDNB conjugate formation at 340 nm. This method yielded an identical  $\beta_{\text{nuc}}$  value for the reaction as when the thiol consumption was monitored. For either method, pseudo-first-order rate constants were deconvoluted with the known concentrations of electrophile or thiol to yield second-order rate constants for each electrophile–thiol pair. For example, with excess electrophile, E, and variable thiol concentration,  $k_{\text{obs}}$  was obtained from slopes of plots of rate vs [thiol]. The bimolecular rate constant,  $k$ , for each pair of thiol and electrophile was then obtained from  $k = k_{\text{obs}}/[\text{E}]$ . Brønsted coefficients,  $\beta_{\text{nuc}}$ , were obtained from plots of second-order rate constant vs thiol  $\text{pK}_a$  for each electrophile.

**Determination of  $\text{pK}_a$  Values of Thiophenols.**  $\text{pK}_a$  values were measured in 10 mM MES buffer containing 0.2 mM  $\text{NiSO}_4$ , 2 mM EDTA, 10% DMF, and 1% EtOH, at pHs ranging from 3 to 10. Thiolate absorbance was measured at the appropriate  $\lambda_{\text{max}}$  as indicated above.  $\text{pK}_a$  values were obtained with the ENZFitter software package assuming a single ionization. The experimentally determined  $\text{pK}_a$  values were (1), 7.4; (2), 7.2; (3), 7.1; (4), 6.9; (5), 6.4; (6) 4.5.

**Synthesis of Product Thiol–CDNB Conjugates.** Synthesis of all thiol–CDNB conjugates was adapted from the method of Koechel and Cafruny.<sup>19</sup> To a solution of  $\text{NaHCO}_3$  (5 mmol) in 50 mL of  $\text{H}_2\text{O}$ , 5 mmol of CDNB was added. The flask was flushed with argon, followed by dropwise addition of thiol (5 mmol) in 20 mL of EtOH. The reaction mixture was stirred and purged with argon overnight, during which a yellow precipitate formed. The mixture was acidified with HCl (final pH  $\sim$ 2) and extracted with diethyl ether. The extract was concentrated in vacuo to a yellow solid and recrystallized twice from  $\text{CH}_2\text{Cl}_2$ . Analyses were as follows.

**4-Methoxybenzenethiol–CDNB Conjugate (Product of (1) and CDNB).**  $^1\text{H}$  NMR (acetone- $d_6$ ):  $\delta$  8.99 (1H, d,  $J = 2.5$  Hz), 8.33 (1H, dd,  $J_a = 2.5$  Hz,  $J_b = 9.1$  Hz), 7.62 (2H, d,  $J = 8.7$  Hz), 7.14–7.2 (3H, m), 3.92 (3H, s). FAB-MS: 306 ( $\text{M}^+$ , base), 289 (35.5), 273 (10.2), 259 (8.9), 242 (15.4), 227 (23.0), 196 (30.7).  $\epsilon_{340} = 8500\text{ M}^{-1}\text{ cm}^{-1}$ .

**4-Methylbenzenethiol–CDNB Conjugate (Product of (2) and CDNB).**  $^1\text{H}$  NMR (acetone- $d_6$ ):  $\delta$  8.99 (1H, dd,  $J_a = 2.5$  Hz), 7.58 (2H, d,  $J = 8.1$  Hz), 7.45 (2H, d,  $J = 7.8$  Hz), 7.15 (1H, d,  $J = 9.1$ ), 3.45 (3H, s). EI/MS: (70 eV) 290 ( $\text{M}^+$ , 69.0), 202 (19.6), 197 (27.7), 180 (base), 153 (18.3), 139 (24.8).  $\epsilon_{340} = 9200\text{ M}^{-1}\text{ cm}^{-1}$ .

**4-Hydroxybenzenethiol–CDNB Conjugate (Product of (3) and CDNB).**  $^1\text{H}$  NMR (acetone- $d_6$ ):  $\delta$  8.99 (1H, d,  $J_a = 2.5$  Hz,  $J_b = 8.7$  Hz), 7.52 (2H, d,  $J = 8.7$  Hz), 7.16 (1H, d,  $J = 9.0$  Hz), 7.08 (2H, d,  $J = 8.7$  Hz). EI/MS: (70 eV) 292 ( $\text{M}^+$ , 43.2), 275 (67.5), 200 (23.6), 199 (17.7), 167 (base), 139 (40.1).  $\epsilon_{340} = 9000\text{ M}^{-1}\text{ cm}^{-1}$ .

**Benzenethiol–CDNB Conjugate (Product of (4) and CDNB).**  $^1\text{H}$  NMR (acetone- $d_6$ ):  $\delta$  9.01 (1H, dd,  $J_a = 2.3$  Hz,  $J_b = 9.0$  Hz), 7.74–7.64 (5H, m), 7.16 (1H, d,  $J = 9.1$  Hz). EI/MS: (70 eV) 276 ( $\text{M}^+$ , 41.0), 259 (6.1), 195 (9.1), 183 (18.2), 166 (base), 152 (18.3), 139 (52.3), 77 (37.5).  $\epsilon_{340} = 9000\text{ M}^{-1}\text{ cm}^{-1}$ .

**4-Chlorobenzenethiol–CDNB Conjugate (Product of (5) and CDNB).**  $^1\text{H}$  NMR (acetone- $d_6$ ):  $\delta$  9.01 (1H, d,  $J = 2.5$  Hz), 8.36 (1H, dd,  $J_a = 2.5$  Hz,  $J_b = 8.9$  Hz), 7.77–7.65 (4H, m), 7.24 (1H, d,  $J = 9.01$  Hz). EI/MS: (70 eV) 312 ( $\text{M}^+$ +2, 12.8), 310 ( $\text{M}^+$ , 32.2), 288 (42.6), 286 (56.4), 211 (16.9), 202 (31.0), 200 (80.0), 143 (base), 139 (36.0), 108 (53.2).  $\epsilon_{340} = 9200\text{ M}^{-1}\text{ cm}^{-1}$ .

**4-Nitrobenzenethiol–CDNB Conjugate (Product of (6) and CDNB).**  $^1\text{H}$  NMR (acetone- $d_6$ ):  $\delta$  9.02 (1H, d,  $J = 2.5$  Hz), 8.43 (2H, d,  $J = 9.1$  Hz), 8.36 (1H, dd,  $J_a = 2.4$  Hz,  $J_b = 9.0$  Hz), 8.02 (2H, d,  $J = 8.7$  Hz), 7.390 (1H, d,  $J = 9.0$  Hz). EI/MS: (70 eV) 321 ( $\text{M}^+$ , 86.7), 240 (42.8), 227 (21.1), 211 (93.1), 210 (56.8), 165 (61.7), 153 (53.0), 139 (base), 95 (29.7), 79 (33.0), 63 (62.5).  $\epsilon_{340} = 10\,700\text{ M}^{-1}\text{ cm}^{-1}$ .

**Enzymatic Reactions.** Enzymatic reactions were performed at 25  $^\circ\text{C}$ , in 0.1 M potassium phosphate at the pHs indicated in Results and the figures. Enzymatic activities of wild-type rat GSTA1-1 and site-directed variants for CDNB, EA, and EPNP were determined spectrophotometrically according to Habig et al.,<sup>5a</sup> in the presence of varying concentrations of viscogen. CDNB-dependent reactions contained 1 mM CDNB and 1 mM GSH. EA-dependent reactions contained 0.6 mM EA and 5 mM GSH. For EPNP turnover, reactions contained 5 mM EPNP and 5 mM GSH. Activity with CHP was determined by the method of Lawrence and Burke.<sup>20</sup> With this substrate, reactions contained 1.5 mM CHP, 1 mM GSH, 0.3 units of GSSG reductase (Sigma, St. Louis, MO), and 0.25 mM NADPH. Substrates were added from concentrated stock solutions in EtOH. The final concentrations (v/v) of EtOH in the reaction mixtures were 4% for CDNB and EA and 5% for CHP and EPNP. At each pH and viscogen concentration, it was demonstrated experimentally that the electrophile was at saturating concentration. Solutions contained 0–30% sucrose (w/v). Viscosities were determined with an Ostwaldt viscometer at 25  $^\circ\text{C}$ .  $\text{pK}_a$  values of GSH complexed with each of the proteins studied were determined by UV spectroscopy, monitoring the absorbance at 239 nm, in solutions containing protein and saturating GSH as described previously.<sup>4c</sup>

**Acknowledgment.** The authors gratefully acknowledge Mike Fisher and Professor William F. Trager for helpful discussions and Dr. Eric C. Dietze for experimental determination of the GSH  $\text{pK}_a$  values complexed with GST mutants. This work was supported by The National Institutes of Health (GM51210 and GM7750) and Merck Research Labs, Rahway, NJ.

JA980816O

(20) Lawrence, R. A.; Burke, R. F. *Biochem. Biophys. Res. Commun.* **1976**, *71*, 952.

(19) Koechel, D. A.; Cafruny, E. J. *J. Med. Chem.* **1973**, *16*, 1147.